CrossMark

Influences of filling abandoned salt caverns with alkali wastes on surface subsidence

Xilin Shi · Yinping Li · Chunhe Yang ·
Yulong Xu · Hongling Ma · Wei Liu ·
Guodong Ji

Abstract Abandoned salt caverns, particularly those that allow free draining of brine, are serious potential causes of subsidence above salt mines. Filling such caverns with alkali wastes may eliminate these troubles. Based on the filling project in Jingshen salt mine of China, the influences of filling abandoned free-draining salt caverns with alkali wastes on surface subsidence are discussed. The deposition characteristics of alkali waste slurry were studied by laboratory simulation tests. It is found that alkali waste slurry has good flowability during injection into a cavern. Based on the results of compression tests under drained conditions, a distribution model of void ratio of sediment is established. A method for determining the ultimate subsidence value is presented based on the distribution model. The relationship of average effective stress and void ratio of the sediment is also established. Further, a method for predicting development process of surface subsidence is presented. Finally, the specific application procedure of the prediction methods is discussed. According to the research results, filling free-draining salt caverns with alkali wastes can restrain surface subsidence successfully. The reasons can be summed up as: Volume convergence of salt caverns slows down after the caverns are filled owing to the supporting effect of alkali wastes on the rock surrounding caverns, and then, subsidence slows down and decreases, and finally, subsidence stops when the fill material is compacted to its compressed limit.

Keywords Salt mine · Surface subsidence · Abandoned salt caverns · Free draining of brine · Filling with alkali wastes

X. Shi (✉) · Y. Li · C. Yang · Y. Xu · H. Ma · W. Liu
State Key Laboratory of Geomechanics and Geotechnical Engineering, Institute of Rock and Soil Mechanics, Chinese Academy of Sciences, Wuhan 430071, China
e-mail: xlshi@whrsm.ac.cn

Y. Li
Jiangsu Jingshen Salt Chemical Stock Company Limited, Huaian 223200, China

C. Yang · G. Ji
State Key Laboratory of Coal Mine Disaster Dynamics and Control, Chongqing University, Chongqing 400044, China

Introduction

Thousands of salt caverns have been leached out from salt formations by solution mining. Most of them are used for mining salt minerals. Others are used for storing liquid and gas hydrocarbons (Wang et al. 2013), hydrogen gas (Bauer et al. 2013), CO_2 (Hou et al. 2012), and so on. After these salt caverns are abandoned, they usually are filled with saturated brine and then plugged. Even when these measures are taken, the brine pressure loading on the cavern walls is still lower than the initial stress; hence, volume decrease in caverns continues after the caverns are abandoned. Creep shrinkage of the cavern is deemed as the main and direct reason that causes subsidence and displacement (Bérest and Brouard 2003). The convergence of the cavern gradually transfers to the land surface and then causes surface subsidence, or even surface collapse.

Alkali wastes are solid waste generated in the soda ash industry. The main disposal method for these wastes in China is to heap them on the ground, i.e., land disposal. However, this disposal method not only occupies a large land area, but also threatens the environment, such as by contaminating soil and groundwater.

Fortunately, filling salt caverns with alkali wastes can simultaneously deal with the above problems. It cannot

🖄 Springer

only prevent environmental pollution on the land surface, but also prevent surface subsidence (Langer 1993).

The process of filling an abandoned salt cavern with alkali wastes is shown in Fig. 1. First, the alkali wastes are mixed with saturated brine to make a slurry. Then, the slurry is pumped into the abandoned salt caverns. The excess brine is returned to the surface for reuse.

The earliest publicly reported wastes disposal caverns were located at Holford, England, in the 1950s (Hoather and Challinor 1994). Alkali wastes from the soda ash industry were injected into worked-out solution mining caverns. In the later half century, various kinds of nonradioactive wastes, including alkali wastes, brine mud wastes and industrial waste sand, were injected into abandoned salt caverns. In 1990s, Texas State of USA selected six salt caverns for disposing of nonhazardous oilfield wastes and one cavern for disposing of naturally occurring radioactive wastes (Wareen 2006). Davidson et al. (1997) held a view that the underground backfill made with this method is in a state of fluid or semifluid.

However, there were still only a few researches on the behavior of waste sediment and salt caverns. Several scientists, commissioned by the Department of Energy of the USA, evaluated the suitability, feasibility and legality of disposing nonhazardous oil wastes in salt caverns (Tomasko et al. 1997; Veil 1996a, 1997; Veil et al. 1996b, 1998; Argonne National Laboratory 2003). Many experts on salt mechanics were consulted on the stability and long-term behavior of oilfield wastes disposal caverns. Most experts agreed that the waste pile could not offer structural support until nearly all the pore space was eliminated by creep-induced compaction. And these reports concluded that caverns filled with oilfield wastes presented much less likelihood of leaking than brine-filled caverns. Xu et al. (2012) researched the long-term behavior of wastes
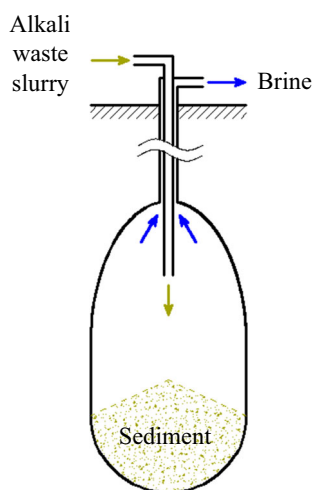
disposal salt caverns and found that the cavern convergence with fluid-bearing backfill was similar with soil consolidation.

Serious surface subsidence or even surface collapse tends to appear more under the condition that brine leaks freely. The reasons for leaking may be that caverns are adjacent to faults, contain nonsalt interlayers, have poor quality cementing or plugging of wells, and so on. The brine in these caverns may leak out freely along some leakage channels. Therefore, the brine pressure cannot increase after these caverns are abandoned. This kind of caverns is defined as "salt caverns losing sealing ability for brine" in the paper. These risky abandoned salt caverns filled with alkali wastes are the study objects of the paper.

Properties of alkali wastes

Physical properties

Alkali wastes are khaki powder, soft and smooth when ground with the fingers. The particle size of alkali wastes is analyzed by Mastersizer 2000 laser diffraction particle size analyzer. As the results shown in Fig. 2, the particle size is less than 200 μm. Their specific surface is 0.68 m^2/g.

The physical indexes of alkali wastes are shown in Table 1. Considering that alkali wastes contain some soluble salt and are hydrophilic, samples are baked for 6 h at 105 °C in a drying oven. Then, the water content is determined. Later, specific gravity of particles is tested with kerosene as neutral medium.

Chemical properties

Chemical compositions are analyzed by Bruker AXS D8-Focus X after alkali wastes being baked for 48 h at 105± 5 °C in a drying oven. The results are shown in
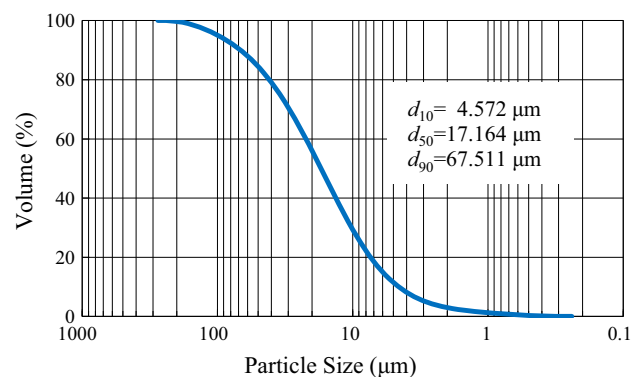

Fig. 1 Process of filling an abandoned salt caverns with alkali wastes

Fig. 2 Particle size gradation curves of alkali wastes

d_{10}= 4.572 μm
d_{50}=17.164 μm
d_{90}=67.511 μm

Table 1 Physical indexes of alkali wastes

Natural water content (%)	Specific gravity of particle	Liquid limit (%)	Plastic limit (%)
103.7	2.56	118.6	89.5

Table 2 Chemical composition of alkali wastes

Component	$CaCO_3$	$CaSO_4 \cdot 0.5H_2O$	NaCl	SiO_2	Mackayite
Content (%)	32.49	62.70	0.04	1.71	3.06
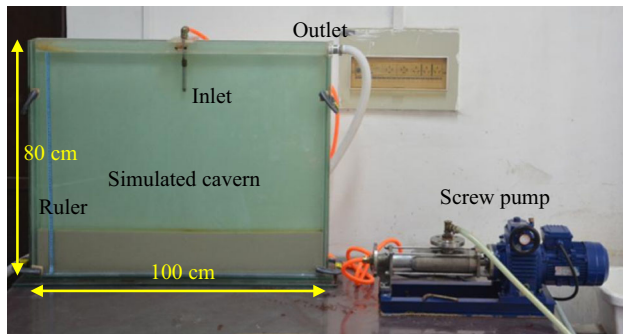
Fig. 3 Two-dimensional simulation device of filling a salt cavern with alkali waste slurry

Table 2. The main chemical components are $CaCO_3$ and $CaSO_4$.

Based on the test results shown in Table 2, alkali wastes have stable chemical properties. No new matter with high mechanical strength is generated in the short term after alkali wastes are pumped in a salt cavern. Fill material in the cavern may be in a form of granular media, which is similar to the view of Thoms (1999).

Migration characteristics of alkali waste slurry in salt caverns

Flow characteristics

According to the technical characteristics of filling salt caverns with alkali wastes, a two-dimensional injecting simulation device has been developed as shown in Fig. 3, which mainly includes a simulated cavern and a screw pump. The simulated cavern with dimensions of 100 cm × 80 cm × 5 cm in length, height and width, respectively, is assembled by 12-mm-thick toughened glass. At the start of a test, the simulated cavern is full of saturated brine. The flux of injected slurry is controlled by a G15-1-type screw pump with adjustable speed motor. The inner diameter of the inlet is 9 mm, and the distance between the inlet and the cavern bottom is 66 cm.

Table 3 Test conditions of injection simulation

No.	Flux (cm^3/s)	Flow velocity (cm/s)	Initial density (g/cm^3)
S1	22	33.9	1.24
S2	45	70.7	1.24
S3	65	102.2	1.24
H1	65	102.2	1.30

As shown in Table 3, four operating conditions are designed based on the range of slurry concentration and flow velocity in practical engineering. The test results have a high reliability because an identical new test had been carried out if some abnormalities were found in a test. Abnormalities usually are brine spill, pump or pipe blockage, inhaling too much air.

It is observed that the phenomena are similar under all test conditions. Taking test No. S2, for example, alkali waste slurry is fast diluted and evenly disperses after being injected into the cavern as shown in Fig. 4. When injecting completely stopped, the alkali waste slurry begins to settle. The trends of sediment interface change in all test conditions are also similar. Still taking test No. S2 as example, as shown in Figs. 5 and 6, sediment height declines mainly in the initial 2 h, and then, the speed of decline obviously becomes slower. Finally, it becomes almost constant.

From the above tests, it is concluded that alkali waste slurry has good flowability during injection into a cavern. Therefore, it can be further inferred that alkali waste sediment in actual salt caverns is uniform in the horizontal directions and has a flat surface, not conical as shown in Fig. 1.

Sedimentation characteristics

The flow tests have given the horizontal distribution characteristics of the sediment. To obtain the distribution characteristics in the vertical direction, settlement tests were performed in a large Plexiglas cylinder, dimensions of which are shown in Fig. 7. Alkali waste slurry with a mass concentration of 10 % is poured into the cylinder until slurry height reaches 180 cm.

The sediment forms and height of alkali waste sediment are shown in Figs. 7 and 8. The height of the sediment surface declines fast in the initial several hours. There is no obvious decline change in the next more than 100 days. Therefore, it can be inferred that the alkali waste slurry should settle out in several hours after being injected into an actual salt cavern.

Compression characteristics of alkali waste sediment

Effective stress with a range of 0–25 kPa

To investigate the compression characteristics of alkali waste sediment, the sediment test in the large Plexiglas cylinder is
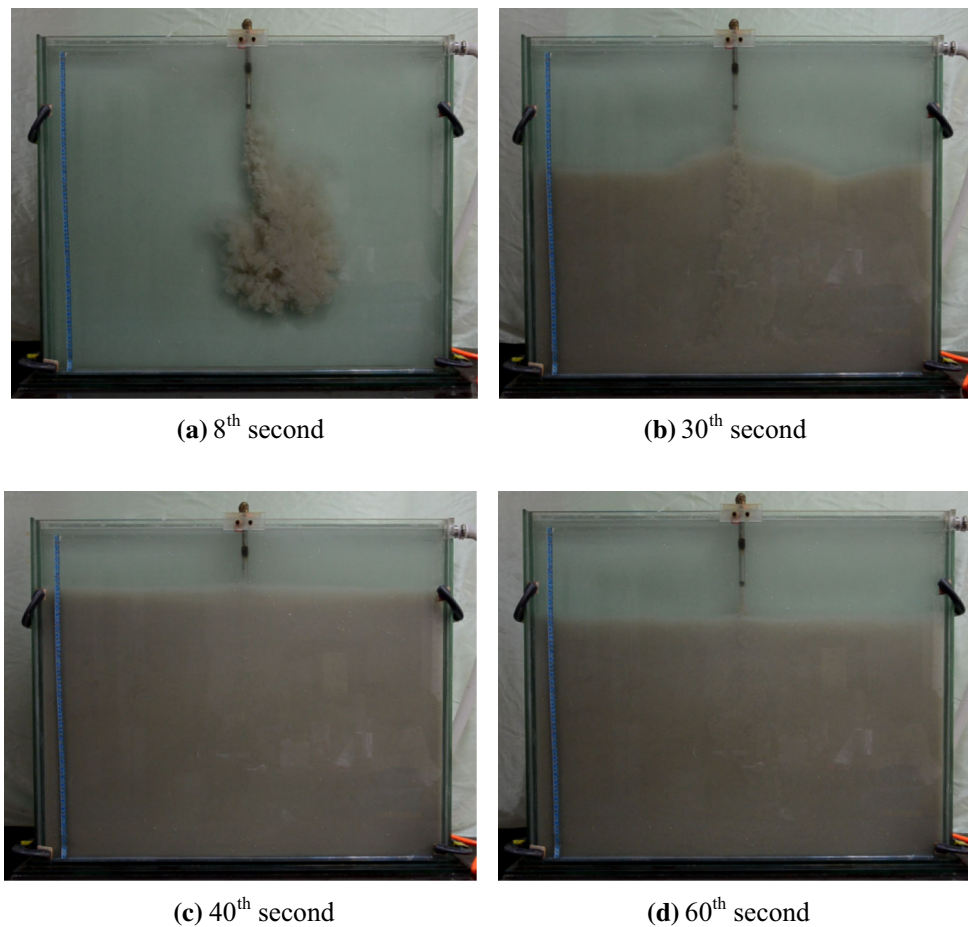
(a) 8ᵗʰ second

(b) 30ᵗʰ second

(c) 40ᵗʰ second

(d) 60ᵗʰ second

Fig. 4 Flow pattern observed when injecting alkali waste slurry into cavern

carried out under effective stresses of 0–25 kPa. The effective stresses are applied by the weights on the surface of the sediment as shown in Fig. 9. Every weight with mass of 19 kg provides 5 kPa effective stress. A porous disc is developed after several repeated trials for the purpose of applying stress uniformly and ensuring brine can drain freely from the sediment pores. As shown in Fig. 8, two pieces of circular Plexiglas plate are assembled with a steel rod, which prevents generating an eccentric force. Filter papers and geotextile are put between porous disc and sediment surface to avoid solid particles escaping from some gaps.

The effective stresses applied, respectively, are valued as 5, 10, 15, 20 and 25 kPa. In every stress step, the judgment criterion for stopping sedimentation is that settlement velocity of the sediment surface is less than 0.001 mm/h. As shown in Fig. 10, the sediment skeleton becomes more and more compacted with the increase in effective stress. Moreover, with the increase in the effective stress, the settlement decrement becomes less and less under the same effective stress increment.

Effective stress with a range of 0–3200 kPa

The height of a salt cavern in practical engineering is usually several tens to hundreds of meters. The effective stress applied on the sediment on the bottom of a salt cavern can reach several MPa. In order to deeply explore the compression characteristics of alkali waste sediment, considering the gradual sedimentation process of alkali wastes, compression tests of alkali waste sediment under drained condition were carried out.

First, compression tests under effective stress 0–20 kPa were carried out in the consolidometer developed by the authors as shown in Fig. 11a. Samples were taken after consolidation was finished. Then, compression tests under effective stress 20–3,200 kPa were carried out in a traditional consolidometer as shown in Fig. 11b.

The curve of void ratio of sediment versus vertical effective stress is shown in Fig. 12. The data in the figure will be used in Sect. 5.1.2 and 5.2.1.
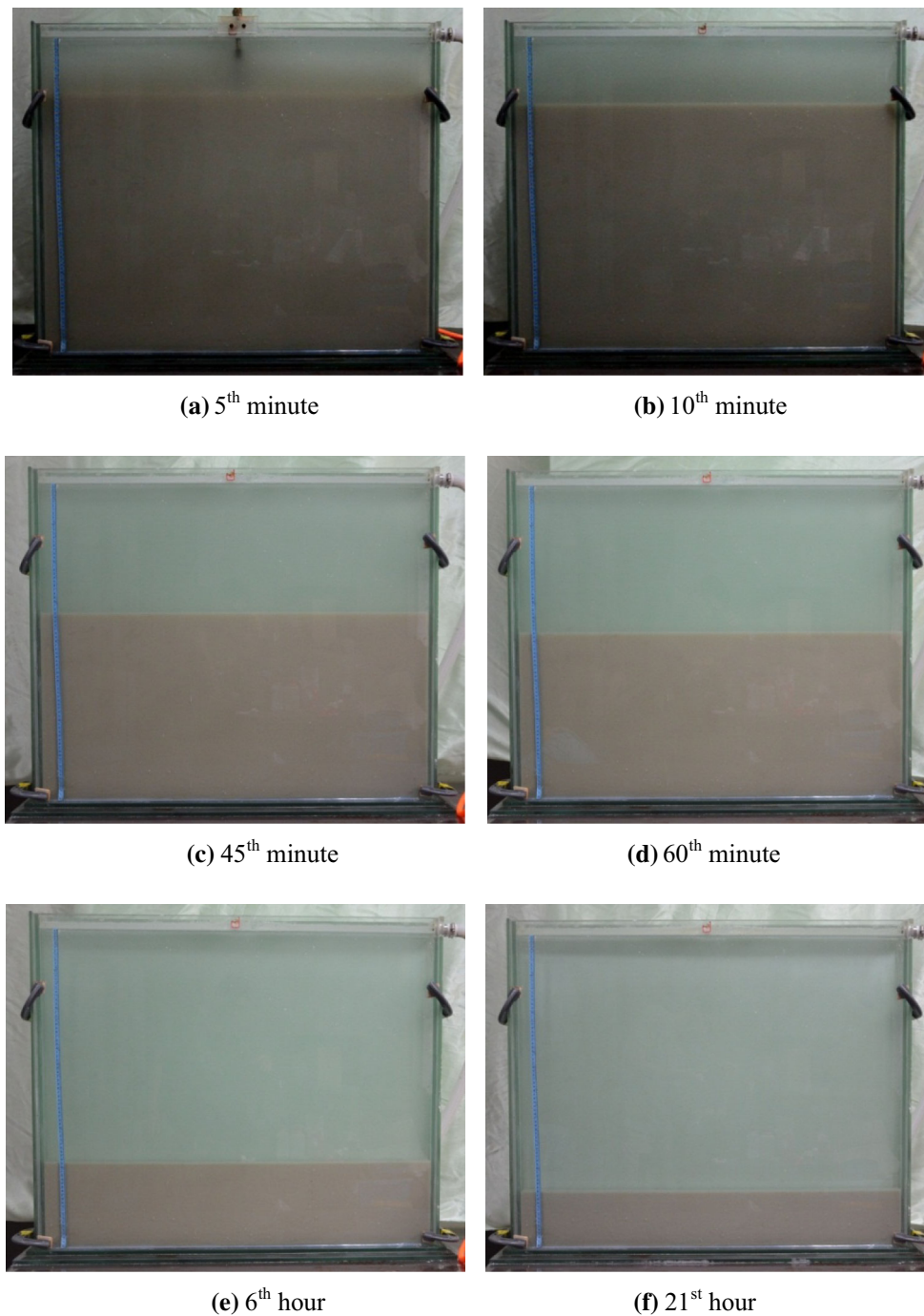
(a) 5th minute

(b) 10th minute

(c) 45th minute

(d) 60th minute

(e) 6th hour

(f) 21st hour

Fig. 5 Sedimentary process after injecting alkali waste slurry

Prediction methods of surface subsidence

Prediction of ultimate subsidence value

Prediction principle

Pore spaces in sediment gradually close following brine leaking and volume convergence of brine free-leaking salt caverns. Based on the assumption that the solid particles of alkali wastes are incompressible, the volume of the sediment will not decrease any more after all pore spaces are closed. At this point, salt cavern shrinkage is restrained and surface subsidence stops.

In practical filling engineering, the total mass of alkali wastes can be obtained by monitoring data. Therefore, the ultimate compressed volume V_{min} can be obtained by
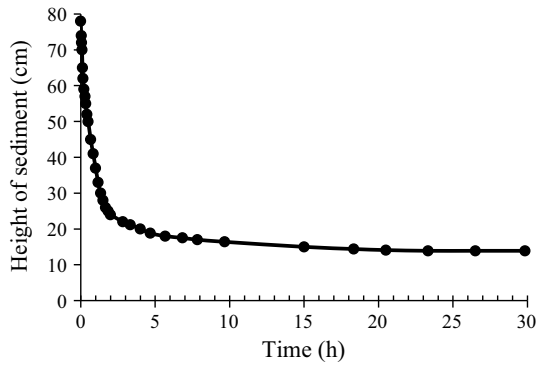
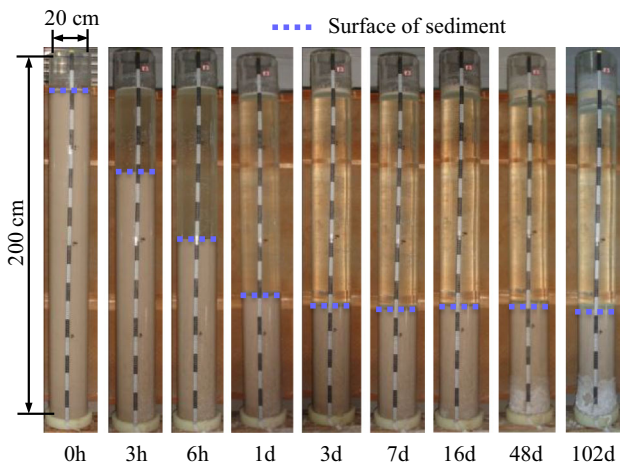**Fig. 6** Heights of sediment versus time after injecting slurry into cavern

0h 3h 6h 1d 3d 7d 16d 48d 102d

Fig. 7 Sediment forms of alkali wastes at different times

$$V_{min} = \frac{m_{dry}}{\rho_{max}} \tag{1}$$

where ρ_{max} is the density of the solid particles, which can be measured by specific gravity test, m_{dry} is the total mass of alkali wastes without water, which can be calculated by records on site.

In evaluation of the prospective effects of a filling project, the ultimate compressed volume V_{min} can be obtained by

Fig. 9 Method to apply effective stress

$$V_{min} = V_{solid} = \int_0^{h_{max}} \frac{1}{1 + e(h)} \pi R^2(h) dh \tag{2}$$

where V_{solid} is the volume of solid particles, h is the distance from top surface to a certain depth of sediment, $R(h)$ is the radius of the salt cavern at depth h, $e(h)$ is the void ratio of the sediment at depth h.

In the following, $e(h)$ will be established based on the test results.

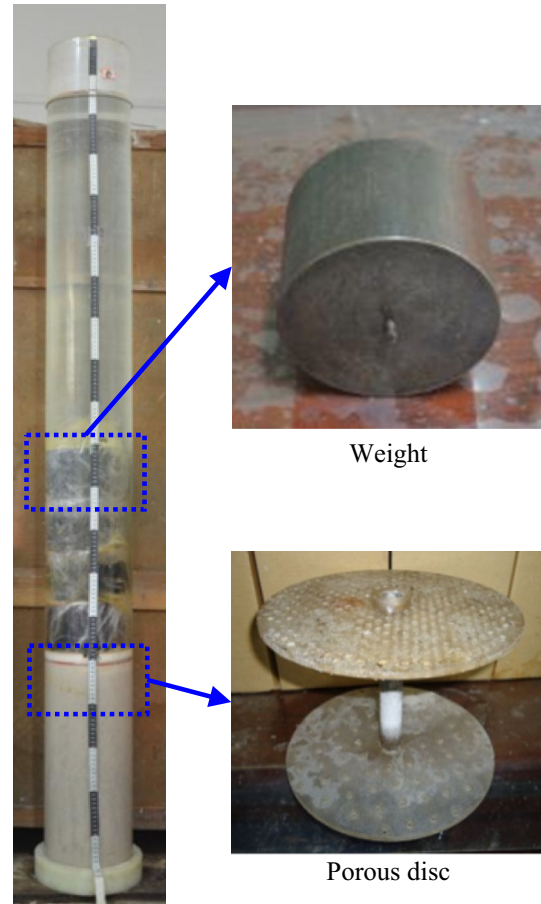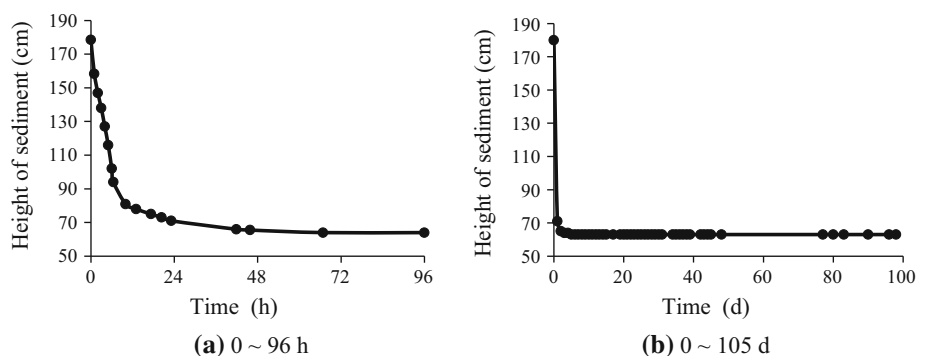**Fig. 8** Heights of sediment versus test time
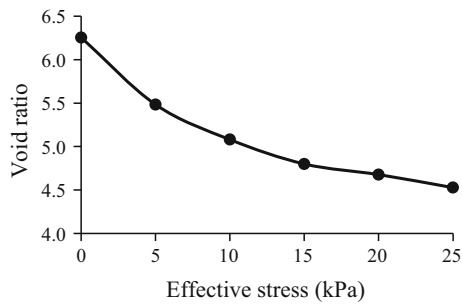

(a) 0 ~ 96 h

(b) 0 ~ 105 d

Fig. 10 Void ratio versus vertical effective stress (0–25 kPa)

Distribution model of void ratio

Taking the sediment with thickness dh at h as the research object, effective stress p applied on the sediment dh is caused by its overlying sediment without brine buoyancy. Then

$$p = \int_0^h \rho' g dh \tag{3}$$

where ρ' is the buoyant density of sediment in brine, g is the acceleration of gravity.

The buoyant density of sediment in brine ρ', which is the difference between sediment density and brine density, can be obtained by

$$\rho' = \rho_{sediment} - \rho_{brine} = \frac{\rho_{brine}e + \rho_{alkali}}{1 + e} - \rho_{brine}$$
$$= \frac{\rho_{alkali} - \rho_{brine}}{1 + e} \tag{4}$$

where $\rho_{sediment}$ is the density of sediment, ρ_{brine} is the density of brine, ρ_{alkali} is the density of solid particles, and e is the void ratio of the sediment.

The densities of the sediment under different effective stress can be calculated according to Fig. 12 and Eq. (4). It is found that a power function fits the test values well, as shown in Fig. 13.
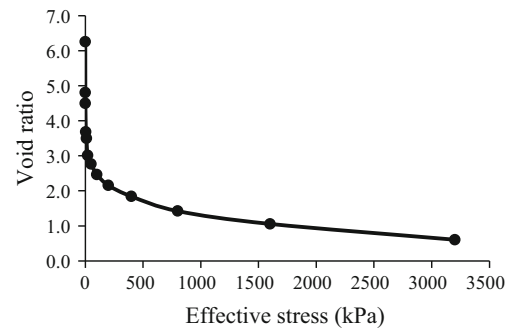

Fig. 12 Void ratio of sediment versus vertical effective stress (0–3,200 kPa)

Therefore, it is obtained that

$$\rho' = a(p - b)^c \tag{5}$$

where the units of ρ' and p are g/cm^3 and kPa, respectively, and $a = 0.14490$, $b = -14.64970$, $c = 0.22072$.

Substituting Eq. (5) into Eq. (3) and considering the boundary condition that $h = 0$ when $p = 0$, it is obtained that

$$p = b + \left[agh(1 - c) + (-b)^{1-c} \right]^{\frac{1}{1-c}} \tag{6}$$

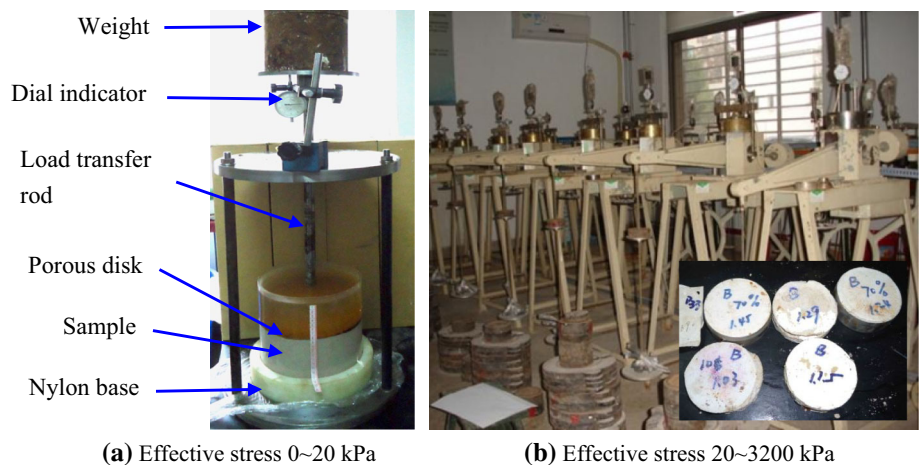Substituting Eq. (6) into Eq. (5), it is obtained that

$$\rho' = a \left[agh(1 - c) + (-b)^{1-c} \right]^{\frac{c}{1-c}} \tag{7}$$

Substituting Eq. (7) into Eq. (4), it is obtained that

$$e(h) = \frac{\rho_{alkali} - \rho_{brine}}{a \left[agh(1 - c) + (-b)^{1-c} \right]^{\frac{c}{1-c}}} - 1 \tag{8}$$

Substituting Eq. (8) into Eq. (2), considering the shape of salt cavern, the ultimate compressed volume V_{min} of the sediment can be obtained.

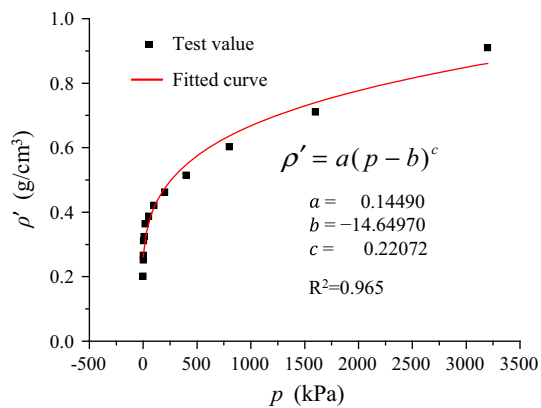Fig. 11 Compression test devices for testing under drained condition

Weight
Dial indicator
Load transfer rod
Porous disk
Sample
Nylon base

(a) Effective stress 0~20 kPa   **(b)** Effective stress 20~3200 kPa

Fig. 13 The fitted curve of buoyant density ρ' and effective stress p

Prediction of subsidence development

The deformation of alkali waste sediment in abandoned salt caverns is essentially a process of being compacted gradually under effective stress. So, the restriction effects of fill material on surface subsidence are due to the supporting effect of the fill material and the brine on the rock surrounding the salt cavern. The brine pressure can be obtained easily for the salt caverns under the condition of brine leaking freely. Therefore, the development process can be well predicted if the relationship of effective stress and volume of sediment is established.

Relationship of effective stress and void ratio

The relationship of effective stress and void ratio could be established by the equations of Sect. 5.1.2. However, the equations mainly represent the relationships of pressure and void ratio of sediment under natural sedimentation. And also, the equations are too complex to apply to numerical simulation. On account of these problems, a new relationship will be established following the Cam-Clay model of soil.

The flow test results indicate that alkali waste slurry has good flowability. So, it is reasonable to assume that principal stresses in three dimensions are equal in the compression process. Therefore, based on the relationship of void ratio and effective stress as shown in Fig. 12, it is obtained that

$$\bar{e} = \alpha - \beta \ln \sigma' \tag{9}$$

where $\bar{e}$ is the average void ratio of the sediment, σ' is the average effective stress with unit kPa, $\alpha = 6.9358$ and $\beta = 0.3967$ are obtained by fitting the test data.

Then, it is obtained that

$$\sigma' = \exp\left(\frac{\alpha - \bar{e}}{\beta}\right) \tag{10}$$

Based on Eq. (10), effective stress σ' can be obtained by monitoring volume convergence of salt caverns in numerical calculation.

Prediction procedure

The prediction procedure of the numerical calculation based on the effective stress principle is shown in Fig. 14. In the figure, $\bar{e}$ is the average void ratio of the alkali waste sediment, σ_n is the normal stress applied to the rock surrounding the salt cavern, σ', which can be obtained by Eq. (10), is the average effective stress applied on the sediment. P_{brine} is the average brine pressure in the salt cavern. As mentioned in the introduction of this paper, the brine pressure in the free-draining salt caverns cannot increase after they are abandoned. So P_{brine} is a constant for a specific cavern.

Influences of filling on surface subsidence

Numerical simulation conditions

The salt cavern involved in the numerical simulation is located in a salt mine in Jiangsu province, China. The boundaries of the cavern are simplified in the simulation as shown in Fig. 15. Following the symmetry conditions, the cavern is modeled using quarter vertical symmetry. The 3D numerical model is shown in Fig. 16. The origin point (0, 0, 0) of the coordinates is located at wellhead on the surface. The distance between two neighboring caverns usually is 300–400 m in the mentioned salt mine. Taking into account neighboring caverns, the distance from the axis to the outer radius is selected as 350 m. The depth range of mudstone is 0–500 m, and the depth range of rock salt is 500–1,150 m. The normal displacement of the surface of the model is fixed except on the surface. The initial stress field is a hydrostatic pressure field caused by rock gravity. Assuming that the saturated brine in the cavern can leak out freely after the cavern is abandoned and that the hydraulic head of the brine pressure is located on the surface, the average brine pressure $P_{\text{brine}} = (1.2 \times 10^3 \text{ kg/m}^3) \times (9.8 \text{ N/kg}) \times ((835 \text{ m}+924 \text{ m})/2) = 10.3 \text{ MPa}$.

Creep material model of salt is cpower (Itasca 2005). The viscoplastic model cpower combines the behavior of the viscoelastic Norton power law and the Mohr–Coulomb elastoplastic model. In the model formulation, the total strain rate $\dot{\varepsilon}_{ij}$ is decomposed into elastic ($\dot{\varepsilon}_{ij}^e$), viscous ($\dot{\varepsilon}_{ij}^c$) and plastic ($\dot{\varepsilon}_{ij}^p$) components:
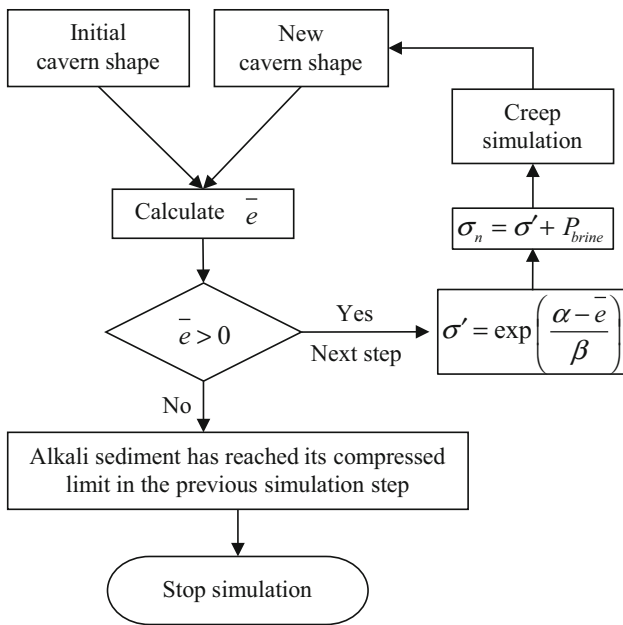
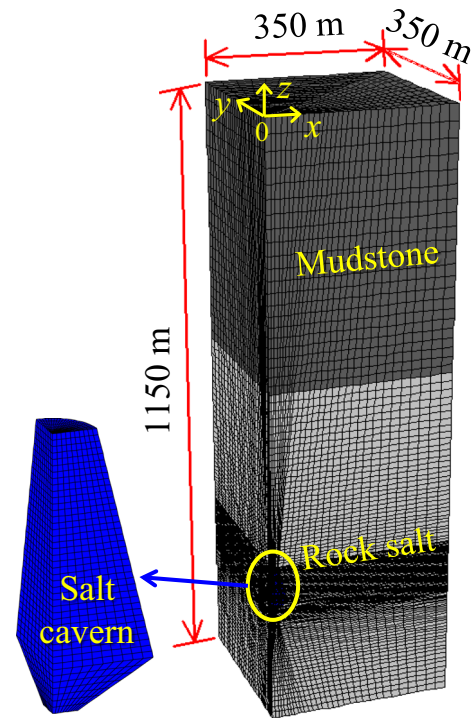Fig. 14 Flowchart of predicting development of subsidence by numerical simulation
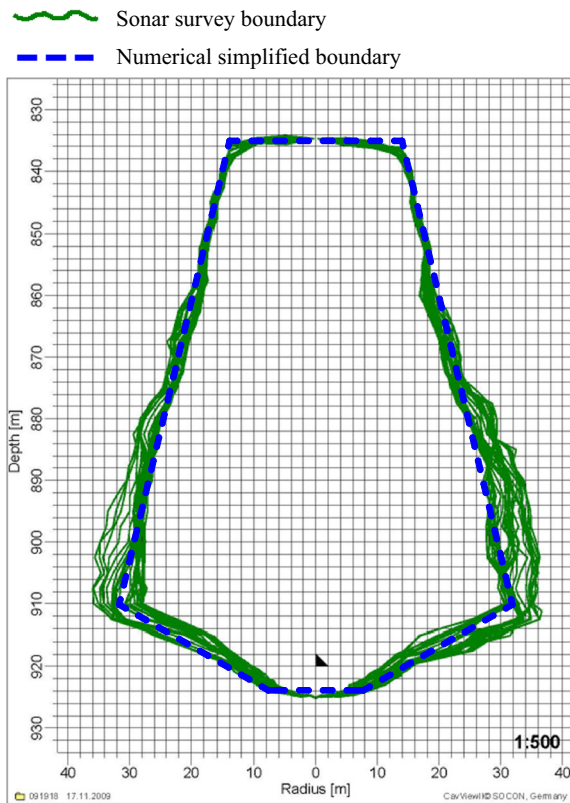

Fig. 15 Sonar survey and numerical simplified boundaries of salt cavern CXI-1

Fig. 16 The 3D numerical model of salt cavern CXI-1

$$\dot{\varepsilon}_{ij} = \dot{\varepsilon}_{ij}^{e} + \dot{\varepsilon}_{ij}^{c} + \dot{\varepsilon}_{ij}^{p} \tag{11}$$

Creep is activated by the von Mises stress $q = \sqrt{3J_2}$ in accordance with Norton power law ($J_2 = 1/2 S_{ij}S_{ij}$ is the second invariant of stress deviator tensor), and the creep rate is

$$\dot{\varepsilon}_{ij}^{c} = \dot{\varepsilon}_{cr} \frac{\partial q}{\partial S_{ij}} \tag{12}$$

The direction of creep flow is derived from the definition of q:

$$\frac{\partial q}{\partial S_{ij}} = \frac{3}{2} \frac{S_{ij}}{q} \tag{13}$$

The Norton power law (Norton 1929) is commonly used to model the creep behavior of salt. The standard form of this law is

$$\dot{\varepsilon}_{cr} = Aq^{n} \tag{14}$$

where $\dot{\varepsilon}_{cr}$ is the creep rate, A and n are material properties.

According to the results of rock mechanics tests about the salt mine (Yang et al. 2009), material properties in numerical simulation are listed in Table 4.

Two types of numerical simulation were carried out in order to compare the differences between filled and unfilled caverns. According to the idea shown in Fig. 14, some

special code segments in FLAC3D were written in the FISH language for numerical simulation of the cavern filled with alkali wastes.

The displacements of several nodes on the cavern wall are monitored during simulation. The cavern volumes at different time are obtained by integral computation based on these node displacements. Then, the curves of volume convergences at different time can be drawn. The vertical displacements of points on the ground surface, from which the surface subsidence values can be obtained, are also monitored during the simulations.

Simulation results of surface subsidence

As an example, displacement contours of rock surrounding an unfilled cavern after having been abandoned for 400 years are shown in Fig. 17. At that time, the maximum displacement reaches up to 10 m, which indicates that the cavern volume convergence has been very large (about 60 %).

The subsidence on the surface above an unfilled cavern 400 years after abandonment is shown Fig. 18. It is obvious that the point (0, 0, 0) that is the center of surface has the maximum subsidence, and the farther the distance from center the smaller the subsidence.

The ultimate compressed volume V_{min} can be obtained by Eq. (2). Based on the simplified boundary of the salt cavern in Fig. 15, the $R(h)$ in Eq. (2) is expressed as Eq. (15). The $e(h)$ in Eq. (2) can be obtained by Eq. (8). In Eq. (8), the $\rho_{brine} = 1.2 \times 10^3$ kg/m^3, and the $\rho_{alkali} = 2.56 \times 10^3$ kg/m^3 by the specific gravity of alkali waste particle in Table 1. Based on this information, it can be obtained that the ultimate compressed volume $V_{min} = 4.9 \times 10^4$ m^3. Considering the initial volume of the cavern, which is 15.1×10^4 m^3, the corresponding cavern volume convergence is 67.5 %. The corresponding maximum subsidence is 28 cm as shown in Fig. 19.

$$R(h) = \begin{cases} \dfrac{12}{7}h + 8 & 0 \leq h \leq 14 \\ -\dfrac{6}{25}h + \dfrac{884}{25} & 14 \leq h \leq 89 \end{cases} \quad (15)$$

The progress of surface subsidence above the cavern filled with alkali wastes is shown in Fig. 20. It can be inferred that the subsidence will stop at about the 565th year after filling is finished.
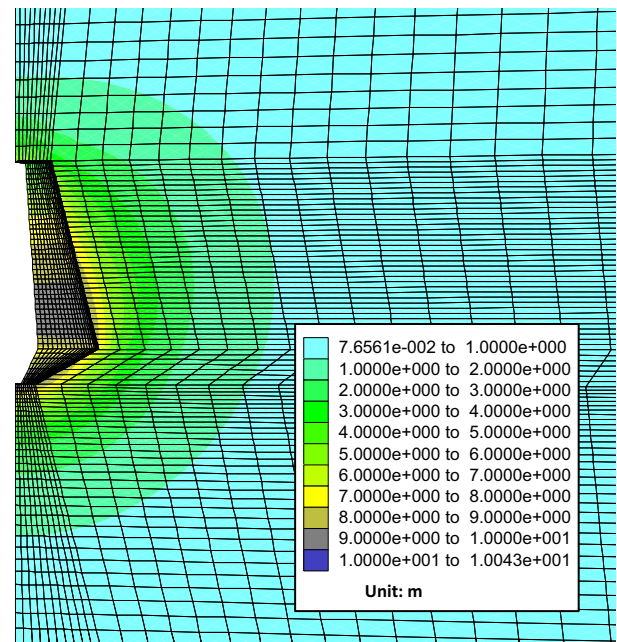

Fig. 17 Displacement contours of rock surrounding an unfilled cavern after having been abandoned for 400 years
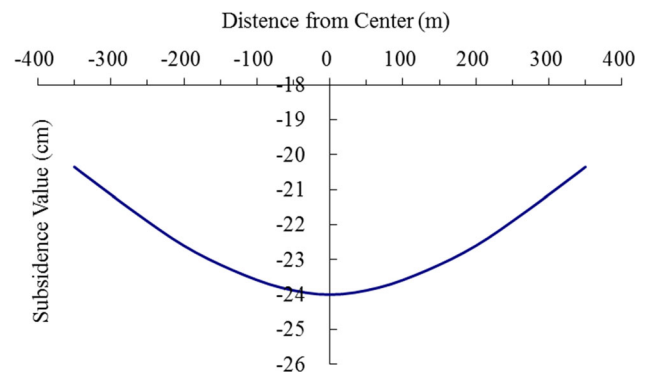

Fig. 18 Subsidence above an unfilled cavern after it has been abandoned for 400 years

Subsidence comparison between filled and unfilled caverns

Volume convergence and surface subsidence comparisons between filled and unfilled salt caverns are shown in Figs. 21 and 22, respectively. The salt cavern closes nearly 1,000 years later if unfilled. However, if filled, surface

Table 4 Material properties in FLAC3D numerical simulation

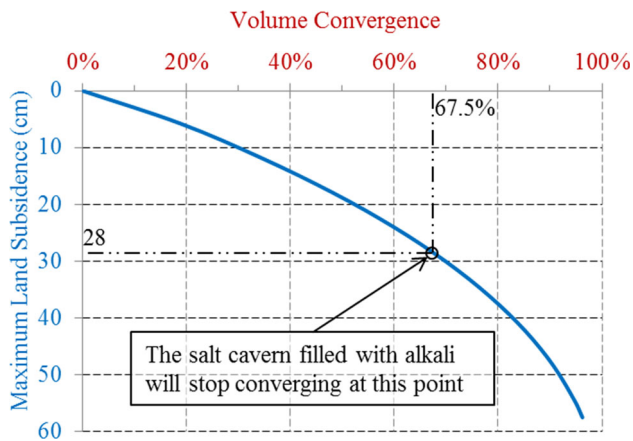| Lithology	Young's modulus (GPa)	Poisson's ratio	Cohesion (MPa)	Internal friction angle (°)	Tensile strength (MPa)	Creep constant n_1	Creep constant a_1 (MPa^{-n-1} year^{-1})
Rock Salt	18	0.30	1.0	45	1.0	3.5	6.0e−6
Mudstone	10	0.27	1.0	35	1.0	–	–

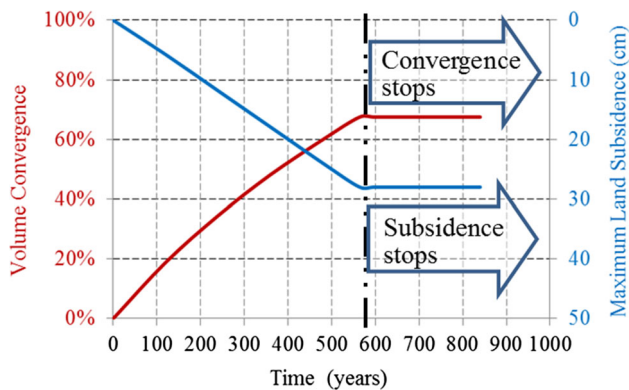**Fig. 19** Ultimate surface subsidence when salt cavern stops converging

Fig. 20 Development of surface subsidence above the cavern filled with alkali wastes
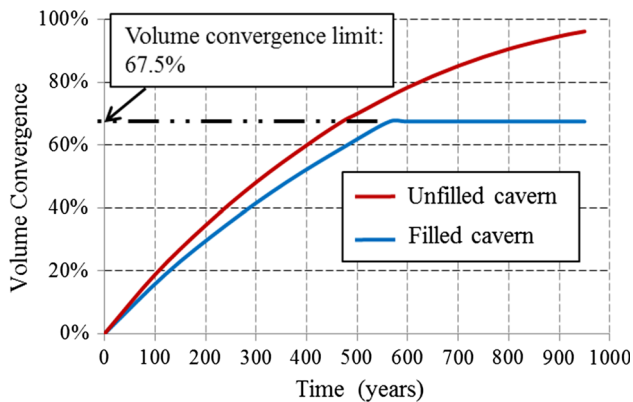

Fig. 21 Volume convergence comparison between filled and unfilled salt caverns

subsidence stops at 28 cm in the 565th year. The ultimate subsidence above a filled cavern is only 49 % of that of an unfilled cavern.
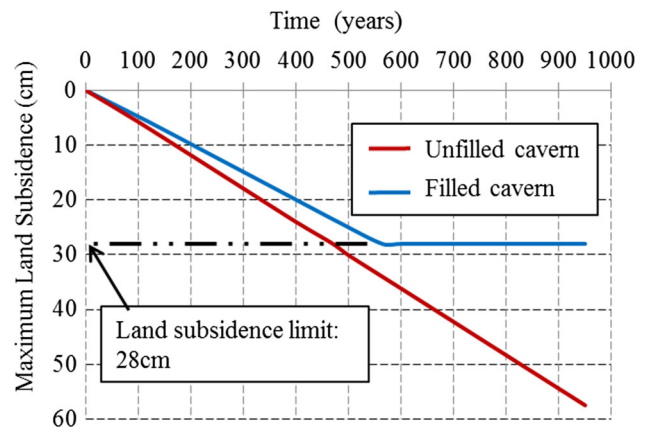

Fig. 22 Surface subsidence comparison between filled and unfilled salt cavern

It is obvious that filling can restrain subsidence above-abandoned salt caverns. As shown in Fig. 23, the reasons can be summed up as: Volume convergence becomes slow after the cavern is filled due to the supporting effect of alkali wastes on the rock surrounding the salt cavern, and then, subsidence becomes slower and smaller, and finally, subsidence stops when the fill material is compacted to its compressed limit.

Summaries and prospects

Summaries

1. By laboratory tests, it is found that alkali waste slurry has good flowability during injection, it also has a very fast sedimentation speed that usually is finished after several hours and alkali waste sediment in salt caverns should be uniform horizontally and have a flat surface.
2. The ultimate subsidence can be predicted based on ultimate compressed volume of alkali wastes. Development of subsidence can be predicted based on the effective stress principle. Prediction of subsidence can be realized with this method under the condition of no constitutive model of fill material being established.
3. Filling salt cavern with alkali wastes can restrain the surface subsidence induced by salt caverns. The reasons can be summed up as: Volume convergence slows after the salt cavern is filled owing to the supporting effect of alkali wastes on surrounding rock, and then, subsidence slows, and subsidence stops when the fill material is compacted to its compressed limit.

Prospects

1. In the actual projects, the alkali waste sediment can have high shear strength when it is compacted to some
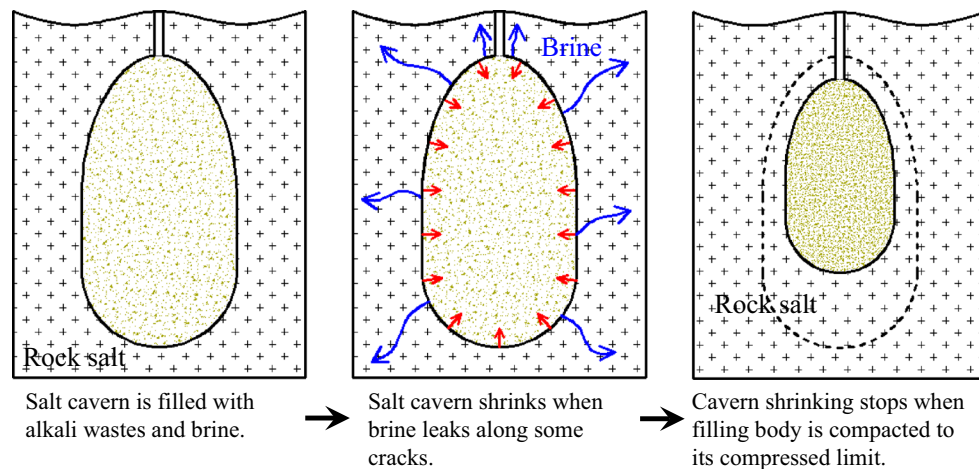
Fig. 23 The restraining process of alkali wastes to the surface subsidence in an abandoned salt cavern

degree, so shear deformation of sediment should be involved in calculation. Therefore, the appropriate constitutive law of alkali waste sediment under high stress state should be established in the further study in order to predict the subsidence process more accurately.

2. From the research results, the total mass of alkali wastes that can be filled in a salt cavern is not very large because of too much pore space in the sediment. In order to increase the total mass of alkali wastes and further restrain cavern convergence, it is valuable to research that mixing some substances can promote the sediment compaction in a short time into alkali waste slurry.

References

Argonne National Laboratory (2003) An introduction to slurry injection technology for disposal drilling wastes. Argonne National Laboratory, Argonne USA

Bauer S, Beyer C, Dethlefsen F, Dietrich P, Duttmann R, Ebert M, Feeser V, Görke U, Köber R, Kolditz O, Rabbel W, Schanz T, Schäfer D, Würdemann H, Dahmke A (2013) Impacts of the use of the geological subsurface for energy storage: an investigation concept. Environ Earth Sci 70(8):3935–3943

Bérest P, Brouard B (2003) Safety of salt caverns used for underground storage. Oil Gas Sci Technol 58(3):361–384

Davidson B, Dusseault MB, Demers R (1997) Solution cavern placement of Solvay process solids—development and implementation of cavern placement technology. In: SMRI Meeting

paper, Fall, 1997. El Paso, Texas, USA. Solution Mining Research Institute

Hoather HA, Challinor D (1994) The use of salt cavities for the disposal of wastes. In: Meeting SMRI (ed) Paper. Solution Mining Research Institute, Hannover

Hou Z, Wundram L, Meyer R, Schmidt M, Schmitz S, Were P (2012) Development of a long-term wellbore sealing concept based on numerical simulations and in situ-testing in the Altmark natural gas field. Environ Earth Sci 67(2):395–409

Itasca (2005) FLAC3D version 3.0 manual. Itasca Consulting Group, Inc, Minneapolis

Langer M (1993) Underground disposal of wastes requiring special monitoring in salt rock masses. In: Proceedings of 3rd Conference on the mechanical behavior of salt. Germany: Clausthal-Zellerfeld Press, pp 583–603

Norton FH (1929) Creep of steel at high temperatures. McGraw-Hill Book Company, New York

Tomasko D, Elcock D, Veil J, Caudle D (1997) Risk analyses for disposing nonhazardous oil field wastes in salt cavern. Report prepared for US Department of Energy

Veil JA (1996) Preliminary technical and legal evaluation of disposing of nonhazardous oil field waste into salt caverns. Final Report. Albuquerque, New Mexico USA: Sandia National Laboratory

Veil JA (1997) Costs for off-site disposal of nonhazardous oil field wastes: salt caverns versus other disposal methods. Report prepared for US Department of Energy

Veil JA, Elcock D, Raivel M, Caudle D, Ayers RC (1996) Preliminary technical and legal evaluation of disposing of Nonhazardous oil field waste into salt caverns. Report prepared for US Department of Energy

Veil JA, Smith KP, Tomasko D, Elcock D, Blunt DL, Williams GP (1998) Disposal of NORM-Contaminated oil field wastes in salt cavern. Report prepared for US Department of Energy

Wang TT, Yan XZ, Yang HL, Jiang TT, Zhao S, Yang X (2013) A new shape design method of salt cavern used as underground gas storage. Appl Energy 104c:50–61

Wareen JK (2006) Evaporites: sediments, resources and hydrocarbons. Springer, New York

Xu YL, Yang CH, Li YP, Guo YT, Ji WD (2012) Preliminary study of the interaction between backfill body and surrounding rock salt mass. In: Bérest P, Ghoreychi M, Hadj-Hassen F, Tijani M (eds) Mechanical behaviour of salt VII. CRC Press, Boca Raton, pp 293–301

Yang CH, Li YP, Chen F (2009) Mechanics theory and engineering of bedded salt rock. Science Press, Beijing (in Chinese)